Vertical stratification-driven nutrient ratios regulate phytoplankton community structure in the oligotrophic western Pacific Ocean

Zhuo Chen[1,3], Jun Sun[2,3*], Ting Gu[3], Guicheng Zhang[3], Yuqiu Wei[4]

[1] College of Biotechnology, Tianjin University of Science and Technology, Tianjin 300457, China;

[2] College of Marine Science and Technology, China University of Geosciences (Wuhan), Wuhan, Hubei 430074, China;

[3] Research Centre for Indian Ocean Ecosystem, Tianjin University of Science and Technology, Tianjin 300457, China;

[4] Yellow Sea Fisheries Research Institute, Chinese Academy of Fishery Sciences, Qingdao, 266071, China

[*]Correspondence: phytoplankton@163.com

Abstract: The stratification of the upper oligotrophic ocean have a direct impact on biogeochemistry by regulating the components of the upper-ocean environment that are critical to biological productivity, such as light availability for photosynthesis and nutrient supply from the deep ocean. We investigated the spatial distribution pattern and diversity of phytoplankton communities in the western Pacific Ocean (WPO) in the autumn of 2016, 2017, and 2018. Our results showed the phytoplankton community structure mainly consisted of cyanobacteria, diatoms, and dinoflagellates, while the abundance of Chrysophyceae was negligible. Phytoplankton abundance was high from the equatorial region to 10 °N, and decreased with increasing latitude in spatial distribution. Phytoplankton also showed a strong variation in the vertical distribution. The potential influences of physicochemical parameters on phytoplankton abundance were analyzed by Structural Equation Model (SEM) to determine nutrient ratios driven by vertical stratification to regulate phytoplankton community structure in the typical oligotrophic ocean. Regions with strong vertical stratification were more favorable for cyanobacteria, whereas weak vertical stratification was more conducive to diatoms and dinoflagellates. Our study shows that stratification is a major determinant of phytoplankton community structure; and highlights that physical process in the ocean control phytoplankton community structure by driving the balance of chemical elements, providing a data base to better predict models of changes in phytoplankton community structure under future ocean scenarios.

Keywords: Vertical stratification; phytoplankton community; western Pacific Ocean; N:P ratio

1. Introduction

Phytoplankton contribute nearly half of global primary production (Field et al., 1998) and represents an important part of biogeochemical cycling and transformation (Falkowski et al., 1998). Marine phytoplankton link the cycling of different elements through their demand for multiple nutrients such as nitrogen (N), phosphorus (P) or iron and their relative availability (Hillebrand et al., 2013). The Redfield ratio is probably the most powerful generalization and cornerstone of the marine biogeochemical cycle (Redfield et al., 1963; Schindler, 2003). The nutrient requirements of phytoplankton are limited by the environmental conditions in which they grow, and nutrient limitation increases the N: P ratio of primary production (Carlson, 2002; Fogg, 1983; Karl et al., 1998). Nitrogen fixation by phytoplankton may deplete phosphorus from the upper ocean, causing an increase to the N: P ratios (Karl et al., 2001). The photosynthesis does not cease, even when there are not enough nutrients to grow (Bertilsson et al., 2003; Geider et al., 1998; Goldman et al., 1979).

Upper-ocean stratification plays an important role in the climate system and in many marine

biogeochemical processes. The degree of vertical mixing is controlled by the strength of nearsurface density stratification (Cronin et al., 2013; Qiu et al., 2004), which impacts the formation of the surface mixed layer (ML) and the entrainment process at the ML's base. The ML depth directly modulates the oceanic reaction to atmospheric forcing and the ocean ventilation process that includes the sinking of water masses into the ocean interior, accompanied by heat, carbon, and oxygen. Upper ocean stratification can directly affect important processes such as biogeochemistry and primary production by regulating the light supply for photosynthesis and nutrient supply from the subsurface ocean (Yamaguchi and Suga, 2019). While the strengthened stratification may produce better light availability for the phytoplankton community, it will also prevent vertical nutrient supply to the euphotic zone from the deep sea (Doney, 2006). Previous studies have shown that net primary production (NPP) shows a stronger linear decrease with stronger vertical stratification and a significant decrease in surface nitrate and phosphate concentrations. The decrease in NPP can be partly explained by the increase in vertical stratification that leads to changes in nutrient concentration (Yamaguchi and Suga, 2019).

In the present study, we focused on the vertical structure of the change in the ocean temperature and salinity, that is, the change in the density stratification. The vertical stratification index (VSI) used in this study is the potential density difference between the surface layer and the depth of 200 meters ($\Delta\rho200$), which can quantify the strength of the upper ocean stratification well (Mena et al., 2019). The purpose of this study is to determine the community composition mechanisms that drive phytoplankton in oligotrophic region. These mechanisms are related to vertical stratification and nutrient ratios. We explored how vertical stratification affects the composition of phytoplankton communities. We hypothesized that vertical stratification might regulate phytoplankton abundance and community composition by driving the ratio of nutrients.

2. Materials and methods

2.1. Study area and sampling

This study relied on the shared voyage of the WPO (0–20 °N, 120–130 °E), commissioned by the National Natural Science Foundation of China. Physical, biological, chemical, and geological surveys were carried out from September to November in 2016, 2017, and 2018 aboard the R/V *Kexue*. The sampling stations used in this study are shown in Figure 1; the sampling layers were 5, 25, 50, 75, 100, 150, and 200 m. Phytoplankton samples from different water layers were placed in 1 L polyethylene bottles, fixed in formaldehyde solution (3%), and stored in dark. Nutrient samples from different layers were placed in PE bottles, frozen, and stored at −20 ℃ for laboratory nutrient analysis.

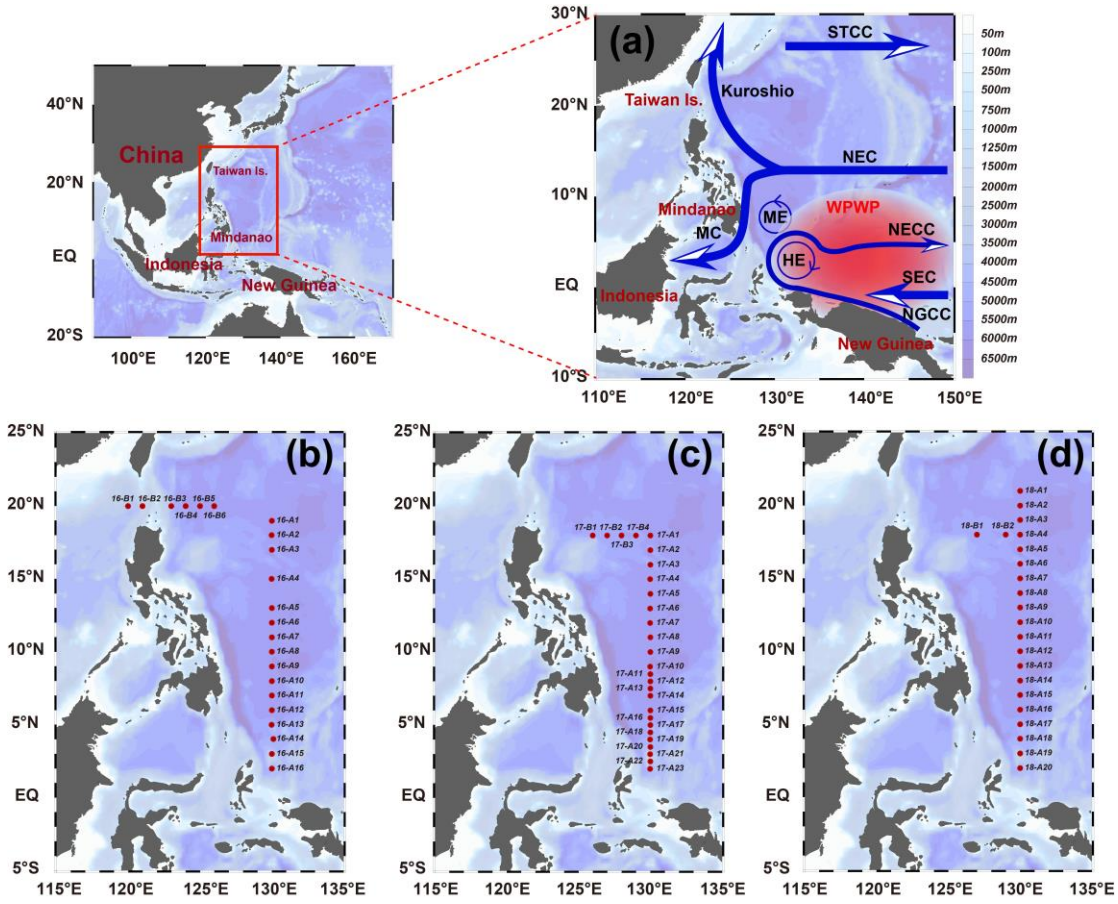

Figure 1. Stations in the western Pacific Ocean (WPO) of three cruises. (a): Current systems of the WPO; (b), (c), and (d): sampling stations of 2016, 2017 and 2018 cruises, respectively. The station at 130°E forms the section A, and the station at 20 °N forms the section B. Map of the WPO shows the major geographic names and the surface currents, including the Subtropical Counter Current (STCC), the North Equatorial Current (NEC), the Northern Equatorial Counter Current (NECC), the South Equatorial Current (SEC), the New Guinea Coastal Current (NGCC), the Mindanao Current (MC), the Mindanao Eddy (ME), the Halmahera Eddy (HE).

2.2. Identification of Phytoplankton

After returning to the laboratory, the Utermöhl method was applied for phytoplankton analysis. A 1 L subsample was allowed to stand for 48 h; then 800 mL supernatant was removed carefully by siphoning through a catheter, taking care to prevent the catheter from touching the bottom of the bottle. Thereafter, the remaining 200 mL liquid was gently mixed and half of which was further concentrated with a 100 mL sedimentation column (Utermöhl method) for 48 h sedimentation (Sun et al., 2002a). The phytoplankton species were identified and enumerated under an inverted microscope (AE2000, Motic, Xiamen, China) at 400× (or 200×) magnification. Phytoplankton identification was conducted as described by Jin et al. (1965), Yamaji (1991), and Sun et al. (2002b), and the World Register of Marine Species (http://www.marinespecies.org). Species identification was as close as possible to the species level. The minimum size of the organisms identified and counted is 20 μm.

2.3. Laboratory Nutrient Analysis

The Technicon AA3 Auto-Analyzer (Bran + Luebbe, Norderstedt, Germany) based on classical colorimetric methods was used for the analysis and determination nutrient (Grasshoff et al., 2009). Soluble inorganic phosphorus (PO_4-P) was determined by the phosphomolybdenum blue method with the limit of detection of 0.02 μmol L^{-1}; dissolved silicate (SiO_3-Si) was determined by the silicon molybdenum blue method with the limit of detection of 0.02 μmol L^{-1}; nitrate (NO_3-N) was determined by the cadmium column method with the limit of detection of 0.01 μmol L^{-1}; nitrite (NO_2-N) was determined by the naphthalene ethylenediamine method with the limit of detection of 0.01 μmol L^{-1} (Dai et al., 2008). Ammonia (NH_4-N) was determined by the sodium salicylate method with the limit of detection of 0.03 μmol L^{-1} (Guo et al., 2014; Pai et al., 2001). Nitrogen-to-phosphorous (N: P) ratio was calculated by dividing nitrogen concentration (NO_3^-+NO_2^-) by phosphate concentration.

2.4. Analysis and methods

A SBE911 CTD sensor and standard Sea-Bird Electronics methods were used to process recorded hydrological parameters. The depth of the mixed layer (ML) is calculated as

$$(S, T)= (Sref, Tref-\Delta T)$$

S and T are the salinity and temperature, respectively, and Sref and Tref are the temperature and salinity at 5 m, ΔT is equal to 0.5 °C.

We calculated the vertical stratification index (VSI) to indicate the degree of vertical stratification of the water column:

$$VSI=\Sigma\ [\delta_\theta(m+1)- \delta_\theta(m)]$$

where δ_θ is the potential density anomaly, and m is the depth from 5 to 200 m.

The abundance of phytoplankton cells in water column was calculated through the trapezoidal integral method (Zhu et al., 2019):

$$P=\left\{\sum_{i=1}^{n-1}\frac{P_{i+1}+P_i}{2}(D_{i+1}-D_i)\right\}/(D_n-D_1)$$

where P is the average value of phytoplankton abundance in water column, P*i* is the abundance value of phytoplankton in layer *i*, *i + 1* is the layer *i + 1*, D*n* is the maximum sampling depth, D*i* is the depth of layer *i*, and n is the sampling level.

We clustered all species based on Bray-Curtis similarity distance the three years, and the results showed four distinct regions using the Primer (version 6). Distance-based Redundancy analysis (db-RDA) and Principal Co-ordinates Analysis (PCoA) were performed using the R package vegan (version 2.5-7) (Oksanen et al., 2020) to explain the relationship between the environmental parameters (temperature, salinity, depth, VSI, Dissolved inorganic nitrogen (DIN) and Dissolved inorganic phosphorus (DIP) and Dissolved silicate (DSi)) and phytoplankton community structure. The results were visualized using the R package ggplot2 (version 3.3.2). SEM was used to assess the relative direct and indirect impact of physical and chemical parameters on phytoplankton abundance. The chi-square test (χ^2), comparative fit index (CFI), and goodness fit index (GFI) were used to assess the model fit.

3. Results

3.1 Hydrographic features of the study area during the sampling years

The surface temperature and salinity of the surveyed sea area in 2016, 2017, and 2018 are shown in Figure 2. In general, the temperature increased with decreasing latitude, and the stations near the equator exhibited the highest temperature; in constrast, the salinity showed an opposite trend as that of temperature, with a high value from 15 °N to 20 °N. The surface temperature (Fig. 2) of the surveyed area in 2016 ranged from 28.58 °C (station 16-B1) to 30.14 °C (station 16-A16), with an average of 29.43 °C. The surface salinity (Fig. 2) of the surveyed area in 2016 ranged from 33.80 (station 16-B2) to 34.65 (station 16-A2), with an average of 34.32. The surface temperature (Fig. 2) of the surveyed area in 2017 ranged from 27.91 °C (station 17-A4) to 30.19 °C (station 17-A20), with an average of 29.26 °C. The surface salinity (Fig. 2) of the surveyed area in 2017 ranged from 33.38 (station 17-A16) to 34.64 (station 17-B4), with an average of 33.94. The surface temperature (Fig. 2) of the surveyed sea area in 2018 ranged from 26.33 °C (station 18-B1) to 29.79 °C (station 18-A17), with an average of 28.83 °C. The surface salinity (Fig. 2) of the surveyed sea area in 2018 ranged from 33.77 (station 18-A14) to 34.64 (station 18-B1), with an average of 34.21.

The profile distribution of temperature and salinity based on the cross-sectional data of different water layers at each station obtained from the survey is shown in Figure 2. The temperature of the shallow water column (0–100 m) is higher than that of the deep-water column (100–200 m). The salinity values of the deep-water bodies (100–200 m) were higher than those of the shallow water bodies (0–100 m). The values of temperature and salinity in 2016, 2017, and 2018 did not change significantly. The temperature of the section in 2016 ranged from 12.16 °C (200 m at station 16-A11) to 30.14 °C (5 m at station 16-A16), with an average of 25.74 °C. The salinity of the section in 2016 ranged from 33.80 (5 m at station 16-B2) to 35.39 (150 m at station 16-A16), with an average of 34.61 °C. The temperature of the section in 2017 ranged from 11.16 °C (200 m at station 17-A13) to 30.19 °C (5 m at station 17-A20), with an average of 25.18 °C. The salinity of the section in 2017 ranged from 33.38 (5 m at station 17-A16) to 35.24 (150 m at station 17-A23), with an average of 34.46. The temperature of the section in 2018 ranged from 9.65 °C (200 m at station 18-A14) to 29.79 °C (5 m at station 18-A17), with an average of 24.22 °C. The salinity of the section in 2018 ranged from 33.77 °C (5 m at station 18-A14) to 35.39 °C (150 m at station 18-A17), with an average of 34.57.

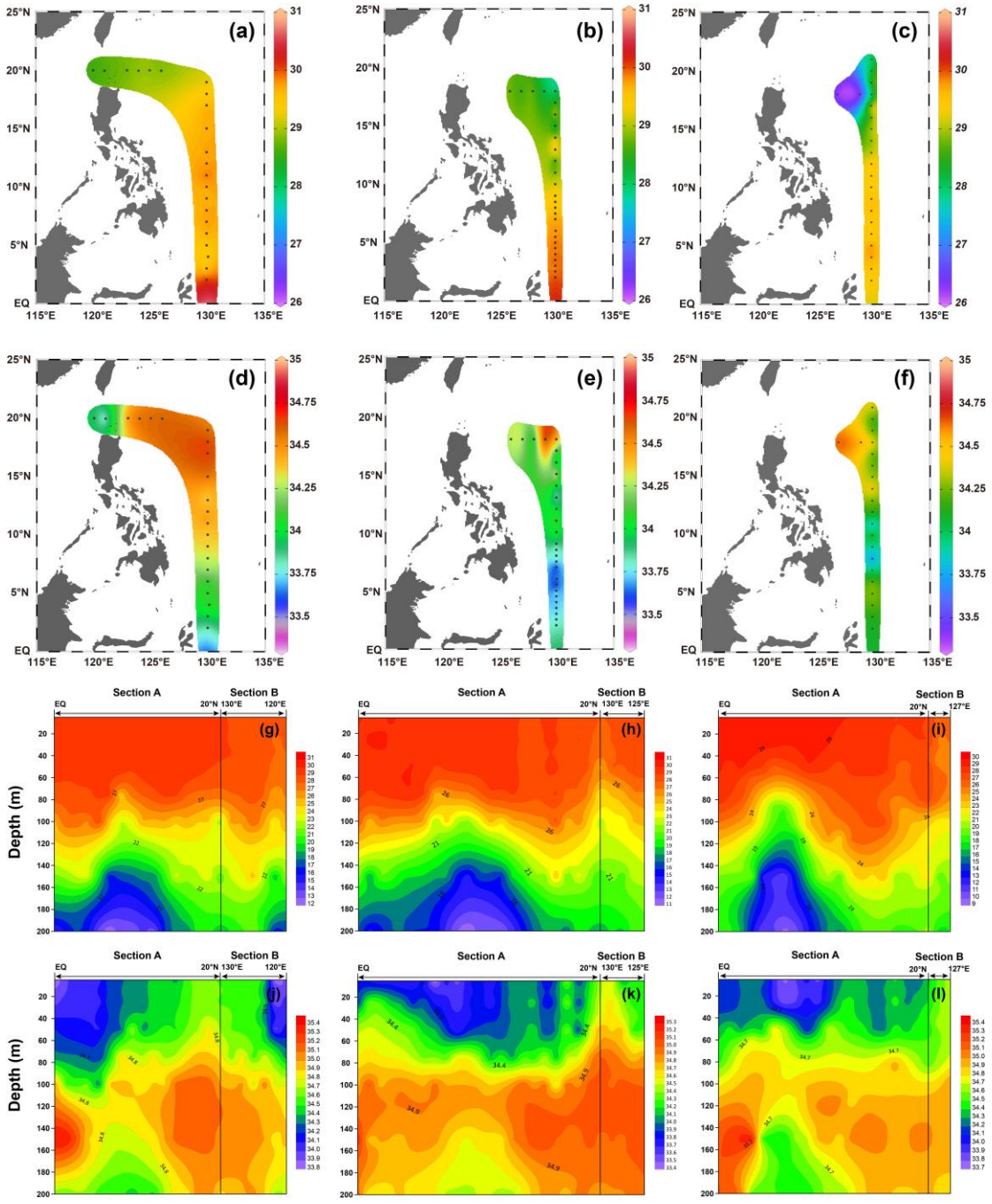

Figure 2. The temperature and salinity distribution in the WPO from three cruises. (a–c) surface temperature in 2016, 2017, 2018 respectively, (d–f) surface salinity in 2016, 2017, 2018 respectively, (g–i) vertical distribution of temperature in 2016, 2017, 2018 respectively, (j–l) vertical distribution of salinity in 2016, 2017, 2018 respectively.

The distribution of the VSI in latitude for the three cruises is shown in Figure 3. Overall, the VSI showed a similar distribution pattern in the three cruises, with the highest value occurring at 7–8 °N and a decreasing trend with increasing latitude. In the 2016 cruise (Figure 3-a), the minimum value of VSI (2.54) appeared in the station at 20 °N (station 16-B4), and the maximum value (4.94) appeared in the station at 7 °N (station 16-A11), with an average of 3.90 ± 0.76. In the 2017 cruise (Figure 3-b), a minimum value of VSI (2.85) appeared in the station at 18 °N (station 17-B4), and

the maximum value (5.54) appeared in the station at 7 °N (station 17-A14) with an average of 4.30 ± 0.82. In the 2018 cruise (Figure 3-c), the minimum value of VSI (2.50) occurred in the station at 18 °N (station 18-B1), and the maximum value (5.48) occurred in the station at 8 °N (station 18-A14) with an average of 4.01 ± 0.95. Interestingly, the VSI varied significantly across latitudinal regions; the VSI was high from the equator to 10 °N, while it was low at 10–20 °N.

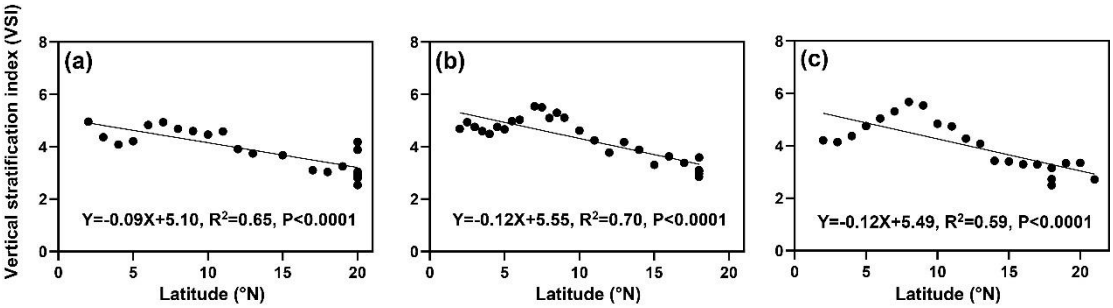

Figure 3. Linear fits of the vertical stratification index with latitude (a) in 2016, (b) in 2017, (c) in 2018. The black dots are the VSI of each station.

3.2 Interannual variation of phytoplankton communities

Figures 4a, b, and c show the horizontal distribution of surface phytoplankton abundance from 2016 to 2018. The interannual variation in phytoplankton was relatively stable, and the sampling area and sampling time from 2016 to 2018 were generally consistent. Most phytoplankton species varied little from year to year in their distribution. Phytoplankton distribution showed a trend of decreasing abundance from the equator to the north with a minor abundance peak at about 10°N. This abundance peak was associated with the predominance of *Trichodesmium*. However, affected by coastal currents, high abundance patches dominated by diatoms were observed also in the Luzon Strait area south of Taiwan, which were carried to the surface by upwelling currents and accounted for more than 67.76% of the abundance at this station. Relatively high abundances were observed at stations in the Kuroshio extension region, consisting mainly of cosmopolitan and warm water species. Phytoplankton abundance was the lowest in the high latitude region.

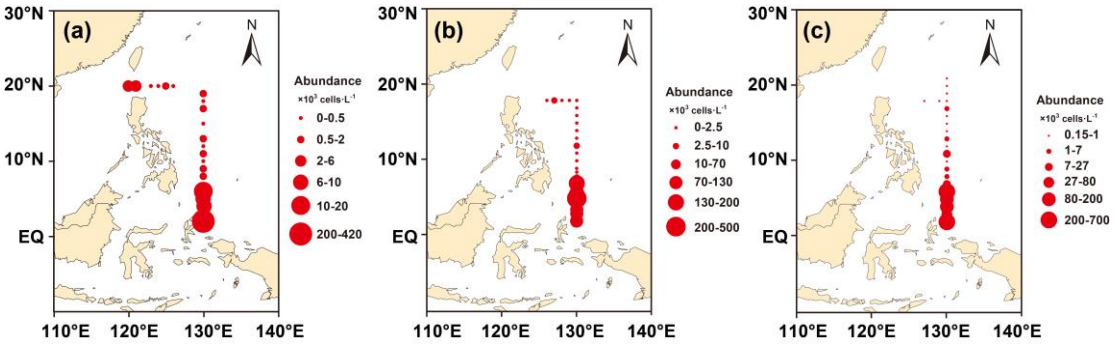

Figure 4. Horizontal distribution of phytoplankton abundance in the WPO. a. 2016, surface layer; b. 2017, surface layer; and c. 2018, surface layer.

3.3 Vertical distribution of phytoplankton abundance

Figure 5 shows the vertical distribution of the phytoplankton. The overall trend in the WPO was consistent across the three cruises in 2016 (a), 2017 (b), and 2018 (c), with the phytoplankton distribution showing variations with latitude and differences in vertical distribution at depth. In

terms of latitude, high phytoplankton value areas were concentrated near the equator (0 °E–8 °E). Vertical distribution of phytoplankton indicated that the plankton-abundant areas occurred from 0–50 m, and the phytoplankton abundance gradually decreased with the increase in depth. Vertical distribution of phytoplankton abundance differed significantly across different areas. In the areas near the equator affected by Halmahera Eddy (HE) and Mindanao Eddy (ME), phytoplankton abundance was mainly concentrated in the upper water column (0–50 m) and consisted mainly of cyanobacteria. In the northern area affected by Kuroshio, the lower phytoplankton abundance was mostly dominated by the equatorial stations, while the phytoplankton species composition was mostly dominated by diatoms and dinoflagellates.

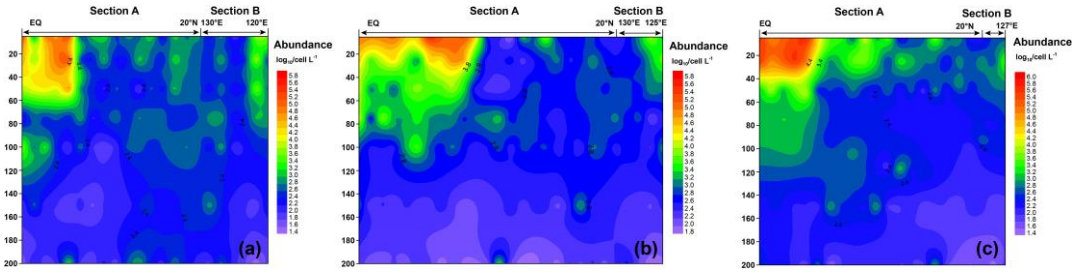

Figure 5. Vertical distribution of phytoplankton abundance (Log10 cells L^{-1}) in the WPO in 2016 (a); 2017 (b) and 2018 (c).

3.4 Phytoplankton community structure

Since there was little interannual difference between species, we clustered all species based on Bray-Curtis similarity distance for stations, and the results showed four distinct regions (Figure 6). Cluster analysis divided the phytoplankton communities at the sampling sites for three years into four groups. Cyanobacteria (>90%) were the dominant species in Groups A and B. The species ratio of diatoms to dinoflagellates in Group A (dias: dinos = 4.8) was higher than that in Group B (dias: dinos = 1.4). Cyanobacteria were the dominant (66%) phytoplankton at the stations of Group C, while diatoms (18%) and dinoflagellates (14%) constituted 32% of the population in this group. Diatoms (43%) and dinoflagellates (49%) dominated the stations in Group D, accounting for approximately 92% of the total phytoplankton. The proportion of Chrysophyceae was low in all four groups (Table 1). The dendrogram showed that these populations were grouped into four groups, which were essentially identical to those determined by PCoA analysis (Figure 7).

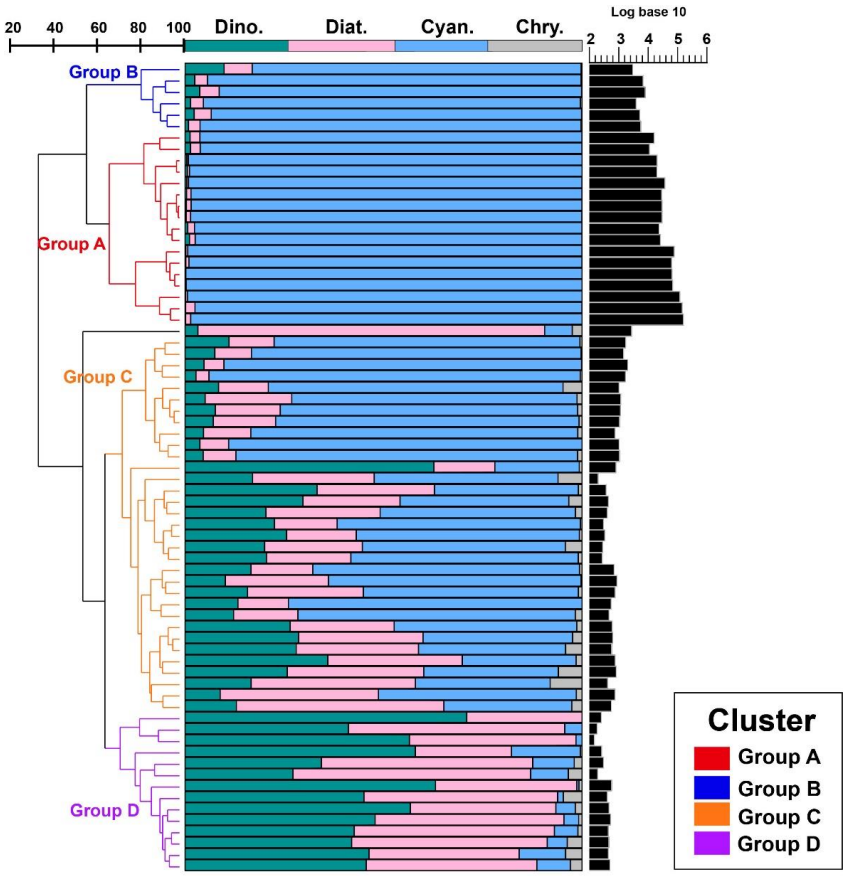

Figure 6. Bray-Curtis similarity-based dendrogram showing averaged phytoplankton community composition and abundance for each station across the 3 cruises. For each station, community composition is indicated with bar plots, and phytoplankton abundance is represented with black bars.

Table 1. The percentages (%) (average ± standard deviations) of diatoms, dinoflagellates, cyanobacteria and chrysophyceae in the four groups.

Species	Group A	Group B	Group C	Group D
Diatoms	1.09±0.79	4.25±1.57	21.83±11.45	43.71±10.12
Dinoflagellates	0.44±0.42	3.41±3.30	17.26±12.45	48.38±11.61
Cyanobacteria	98.45±1.10	92.08±4.79	59.05±20.38	6.06±4.93
Chrysophyceae	0.02±0.01	0.26±0.10	1.86±1.99	1.85±1.66

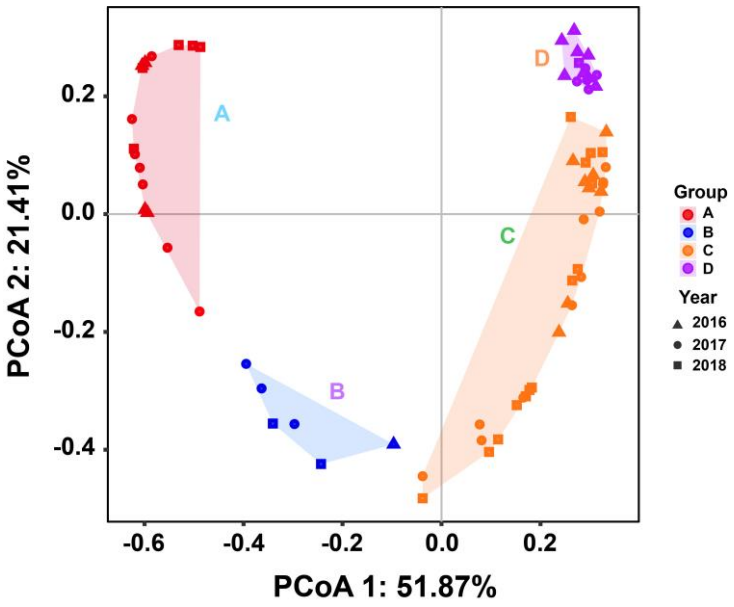

Figure 7. Principal Coordinates Analysis for groups. Triangles, circles, and squares represent 2016, 2017, and 2018 stations, respectively. $P < 0.05$. Different colors represent different groups. Percentages of total variance are explained by coordinates 1 and 2, accounting for 51.87% and 21.41%, respectively.

3.5 Relationships between phytoplankton and environmental factors

The relationship between phytoplankton and environmental factors was analyzed using RDA. We obtained a two-dimensional distribution map of the species, sample distribution, and environmental factors (Figure 8). The results showed that different phytoplankton classes were correlated differently with environmental factors. Cyanobacteria showed negative correlations with temperature and salinity and positive correlations with VSI and nutrient concentration, indicating that waters with high VSI are suitable for the growth of cyanobacteria (mostly *Trichodesmium*). Diatoms and dinoflagellates exhibiting positive correlations with temperature and salinity and negative correlations with VSI and nutrient concentration, indicating that diatoms and dinoflagellates prefer waters with low VSI.

There were four distinct phytoplankton communities in the WPO: Group A was distributed in the equatorial region with clear vertical stratification. This community is characterized by high abundance and is dominated by *Trichodesmium* species such as *T. thiebautii*, *T. hildebrandtii*, and *T. erythraeum*, which are positively correlated with high concentrations of DIN, phosphate, and silicate. Group B was located near 8°N and is mainly influenced by the NECC and mesoscale eddy influence; the phytoplankton community was represented by warm water species, similar to that of Group A. Group C was mainly distributed in the 15 °N region and was strongly influenced by the NEC. Group D was mainly distributed in the 20 °N region, where it was directly influenced by the Kuroshio Current; here, the phytoplankton community was positively correlated with temperature and salinity.

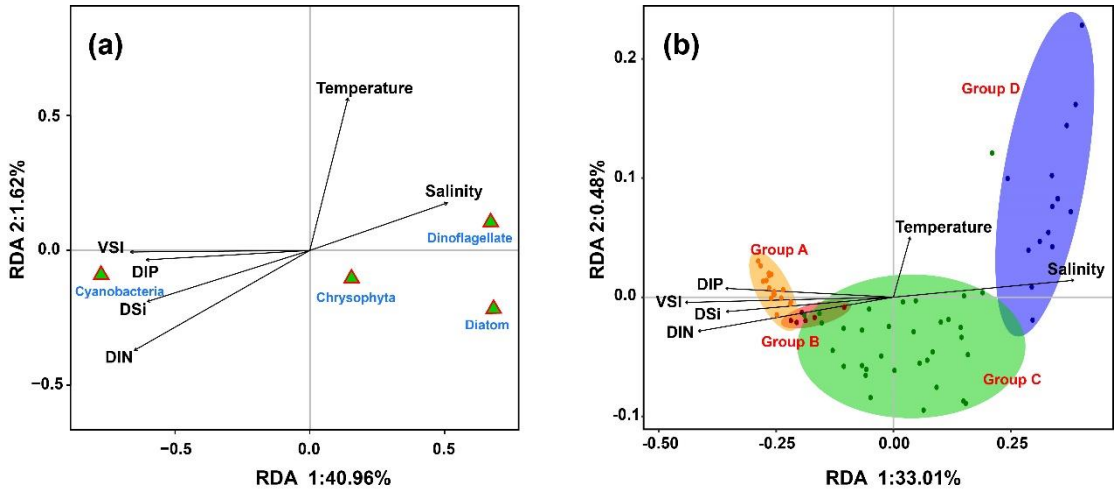

Figure 8. Redundancy analysis of the (a) phytoplankton and environmental parameters, (b) groups and environmental parameters in the WPO. Colored dots represent sampling sites, triangles represent phytoplankton species, and arrows represent environmental factors.

3.6 Temperature, salinity, and vertical stratification index

The temperature, salinity, and VSI of the four groups are shown in Figure 9. The temperature and salinity (T-S) box diagram depicts the four main water masses in the WPO. Groups A (average 29.8 ℃) and B (average 29.6 ℃) had high temperatures, but the salinities of Groups A (average 33.9 ℃) and B (average 33.8 ℃) was low. The temperature of Groups C (average 28.9 ℃) and D (average 28.9 ℃) was low, but the salinity of Groups C (average 34.2) and D (average 34.4) was high (Fig. 9-a). Figure 9 shows clear variation in T-S, we also calculated the vertical stratification index of the four groups (Figure 9-b). Compared with Groups C (average 3.86) and D (average 3.54), the values of VSI in Groups A (average 4.69) and B (average 4.86) were markedly higher, and Group A had the highest VSI. The stratification of the first two groups was more pronounced (Table 2).

The vertical stratification index was related to temperature (Figure 9-a) and salinity (Figure 9-b). Temperature is positively correlated with the vertical stratification index. The VSI of all groups was negatively correlated with salinity. The changes in temperature and salinity were most pronounced in the vertical direction. In Groups A and B with a high stratification index, the changes in temperature and salinity within the group were small. However, the temperature and salinity changed significantly within Groups C and D, with a small stratification index.

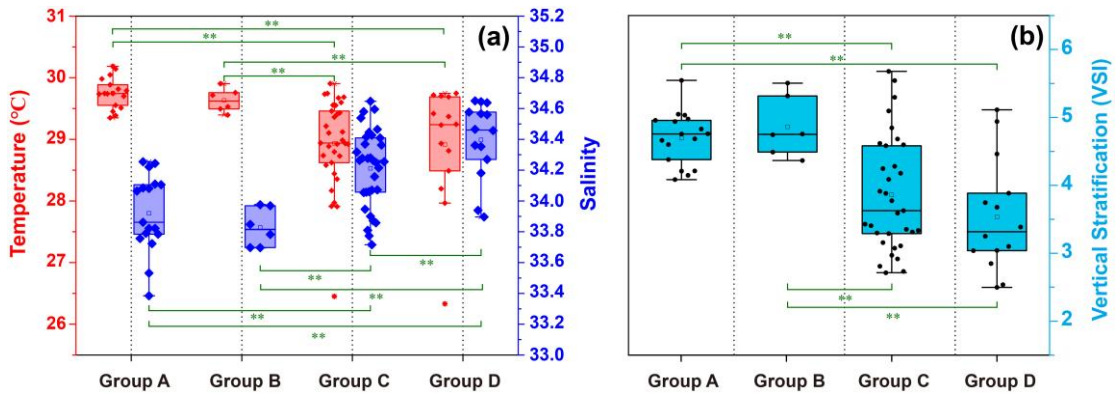

Figure 9 Surface temperature and salinity (a), and vertical stratification index (b) of the four groups.

Table 2. Average (±standard deviations) values for nutrients (μmol L^{-1}), temperature (°C), salinity for each phytoplankton community group were identified by the cluster analysis in the WPO.

	Group A	Group B	Group C	Group D
Temperature	25.30±1.06	24.45±1.85	24.92±1.32	25.41±1.23
Salinity	34.45±0.14	34.40±0.07	34.56±0.16	34.68±0.20
DIP	0.28±0.07	0.18±0.13	0.16±0.13	0.13±0.10
DIN	4.49±1.76	5.43±2.71	2.62±1.89	1.80±1.08
DSi	2.93±1.05	4.13±2.15	1.90±1.47	1.44±0.95
VSI	4.69±0.39	4.86±0.45	3.86±0.84	3.54±0.82

3.7 Direct vs. indirect effects of environmental parameters on phytoplankton abundance

The causal relationships between measured phytoplankton abundance and relevant physical and chemical parameters were examined using SEM, using interactions between temperature, salinity, VSI, DIN, and DIP (Figure 10), as theoretical and experimental data indicated the importance of these variables. The model results showed that temperature, DIP, and DIN had a direct effect on phytoplankton abundance, with temperature having the largest direct effect on phytoplankton abundance (0.38), followed by DIN (0.28) and DIP (0.24). Temperature, salinity, and VSI had indirect effects on phytoplankton abundance, with temperature and salinity having negative indirect effects on phytoplankton abundance (-0.17 and -0.30) and VSI having positive indirect effects (0.31) (Figure 10). From the results of the total effect, only salinity had a negative effect on phytoplankton abundance (-0.30), while both temperature and VSI had positive effects on phytoplankton abundance (0.20 and 0.312), with VSI having the largest total effect. Although the direct effect of temperature on phytoplankton abundance was significant, it was partially offset by the indirect negative effect, while VSI had no direct effect on phytoplankton abundance, but its larger indirect effect resulted in the largest total effect. Both DIN and DIP had positive effects on phytoplankton abundance, but the effect of DIN was greater. Since the vertical distribution of DIN and DIP exhibited stronger variability, more specific analyses of DIN and DIP will be conducted later.

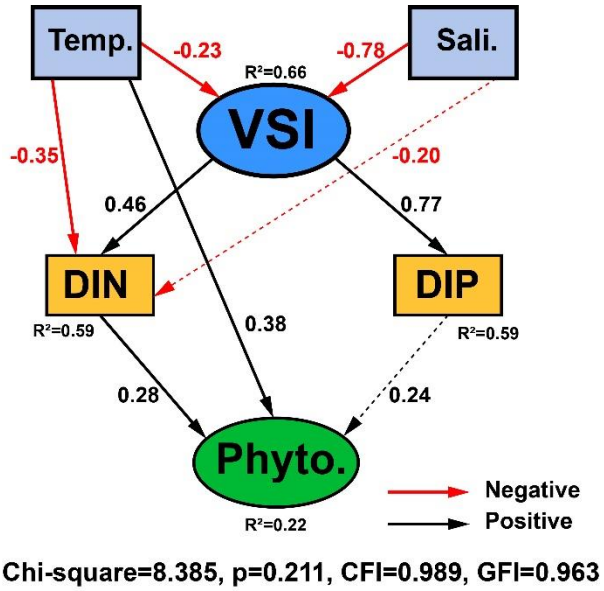

Chi-square=8.385, p=0.211, CFI=0.989, GFI=0.963

Figure 10. Structural Equation Model (SEM) analysis examining the effects of temperature, salinity, VSI, DIN and DIP on phytoplankton abundance. Solid black and red lines indicate significant positive and negative effects at $p < 0.05$, black and red dashed lines indicated insignificant effects. R^2 values associated with response variables indicate the proportion of variation explained by relationships with other variables. Values associated with arrows represent standardized path coefficients.

We analyzed the N:P ratio of the surface layer, SCM, and 200 m. The N:P ratio in the surface layer (N:P>16:1) indicates phosphorus limitation, which is consistent with the SEM analysis (Fig.11). The trophic structure of the SCM layer changed, N:P <16:1 indicated nitrogen limitation, and the depth continued to increase to the bottom of the euphotic layer and stabilized around N:P =16:1, indicating that at the bottom of the euphotic layer, as phytoplankton abundance decreased and interspecific competition decreased, the trophic ratio approached the Redfield ratio and growth may have become increasingly limited by light.

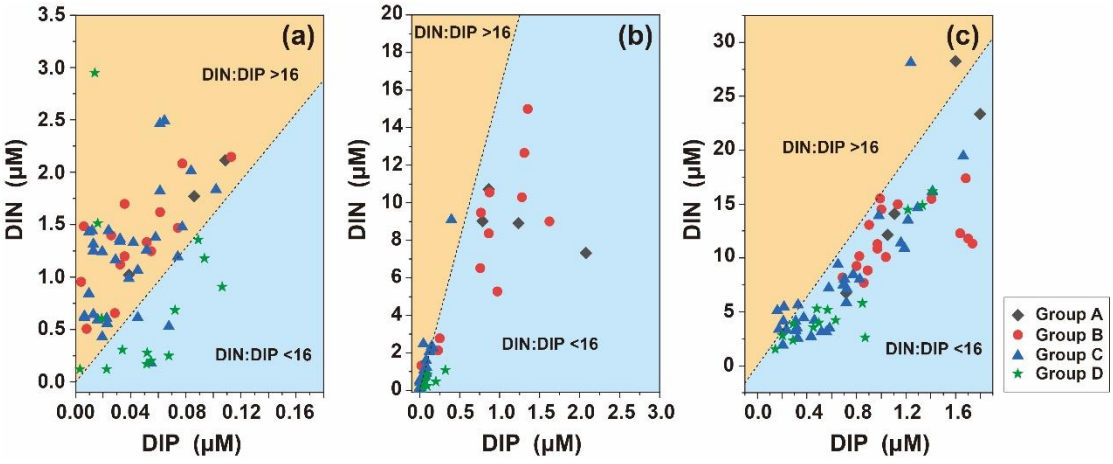

Figure 11. Distribution of phytoplankton community in DIN and DIP. (a): 5 m, (b): SCM, (b): 200 m. The dashed line indicates the Redfield ratio N:P = 16:1.

4. Discussion

4.1 Comparison with historical data

The Kuroshio and WPWP are key areas of the WPO sea-air interaction and climate modulation (Zhang, 1999). Previous surveys have provided less knowledge of the phytoplankton community structure in this study area (Table 3). Previously, samples were collected by net, and net-collected samples reduced phytoplankton abundance in small volumes, thereby underestimating the phytoplankton abundance in the ocean under investigation. In the present study, phytoplankton samples were collected from water samples, which better reflected the phytoplankton community structure and abundance. Sun et al. (2000) and Liu et al. (2000) further investigated the species composition and abundance distribution of phytoplankton diatoms and dinoflagellates in the Ryukyu Islands and nearby waters. Li et al. (2015) conducted a study on phytoplankton in the tropical and subtropical Pacific oceanic zones with response mechanisms to the limitation of nitrogen and iron. Chen et al. (2018a) investigated the phytoplankton community structure and mesoscale eddies in the western boundary current. A total of 199 species in 61 genera belonging to four phytoplankton families were identified, among which the abundance of *Trichodesmium* species

was high. Previous studies have mostly focused on vertical hauls and the horizontal distribution of phytoplankton throughout the water column while ignoring the effect of vertical stratification on phytoplankton.

Table 3. Historical data of the phytoplankton community in the WPO.

Month	Sampling areas	Layer /m	Number of species	Sampling types	References
2018.10	2°–20°N, 120°–130°E	0–200	305	Water samples	This study
2017.10	2°–18°N, 126°–130°E	0–200	339	Water samples	This study
2017.08	10.3°–10.9°N, 139.8°–140.4°E	0–200	147	Water samples	Dai et al.,2020
2017.08	21°–42°N, 118°–156°E	0–200	235	Water and net samples	Lin et al., 2020
2017.05	21°–42°N, 118°–156°E	0–200	248	Water and net samples	Lin et al., 2020
2016.09	2°–21°N, 127°–130°E	0–200	269	Water samples	This study
2016.09	0°–20°N, 120°–130°E	0–200	243	Net samples	Chen et al., 2018b
2014.08	0°–21.5°N, 121°–135.5°E	0–300	199	Net samples	Chen et al., 2018a
1997.07	23°30′–29°30′N, 122°30′–130°30′E	0–200	227	Net samples	Sun et al., 2000
1997.07	23°30′–29°30′N, 122°30′–130°30′E	0–200	251	Net samples	Liu et al., 2000

4.2 Relationship between N:P ratio and vertical distribution of phytoplankton

Research on the factors that control the structure of the phytoplankton community has been carried out for decades, but the hypothesis of nutrient concentration limits and ratios has not been fully explained in terms of affecting the structure of the phytoplankton community (Gao et al., 2019). As diatoms and dinoflagellates show great differences in cell morphology, structure, and nutrition mode, they differ greatly in their nutrient acquisition strategies. Several studies have revealed that dinoflagellates use mixotrophy, engulfing prey as well as feeding using peduncles and palia, while phosphorus limitation is a common factor stimulating dinoflagellates to ingest particulate nutrients (Huang et al., 2005; Smayda, 1997; Stoecker, 1999). The variation in phytoplankton community structure is always correlated with fluctuations in physicochemical environmental parameters.

In the four groups we studied, surface seawater N:P>16:1 indicated that phosphorus in surface seawater was limited, but *Trichodesmium* relied on its own nitrogen fixation function and was highly abundant in oligotrophic waters (Figure 6). The relationship between *Trichodesmium* and nitrogen fixation has already been demonstrated (Grosskopf et al., 2012; Luo et al., 2012; Zehr, 2011). The virtual absence nitrogen limitation in surface seawater in Group D was consistent with the low abundance of *Trichodesmium*, which was consistent with studies on the abundance of *Trichodesmium* in the region (Chen et al., 2019; Sohm et al., 2011). In the WPO, the most oligotrophic ocean around the world (Hansell et al., 2000), nutrients have become an important factor that determines the distribution of phytoplankton. Under nutrition-limited conditions, diatoms and dinoflagellates are more affected, especially under phosphorus limitation (Egge, 1998), which corresponds to the high abundance of Group D diatoms and dinoflagellates. In the present study, the vertical pattern of N: P ratios indicated differences in nutrient composition along the vertical gradient. The N: P ratio of the surface layer (N: P>16: 1) indicates phosphorus limitation, the structure of nutrients in the SCM layer changed, and (N: P<16: 1) indicates nitrogen limitation: the depth continued to increase to the bottom of the euphotic layer and was stable near (N: P=16: 1),

indicating that at the bottom of the euphotic layer, with decreasing phytoplankton abundance, interspecific competition is reduced as light limitation kicks in, and the nutrient ratio approaches the Redfield ratio. The differences in nutrient ratios thus affect the vertical distribution patterns of phytoplankton abundance. Diatoms have higher phosphorus requirements than other phytoplankton groups, which may be reflected by the lower N: P ratio in diatoms than in other groups (Hillebrand et al., 2013). Iron is essential for the synthesis of nitrogen-fixing enzymes in *Trichodesmium*, and *Trichodesmium* have a higher demand for iron than other planktonic organisms. The main source of iron in open ocean is atmospheric deposition. Duce et al. showed that the flux of iron deposition is higher in the WPO, so iron is an important environmental limiting factor for the growth of *Trichodesmium* after temperature (Duce and Tindale, 1991). And we suggest that some of the sampled phytoplankton may have recently sunk from the upper layers and therefore represent nutrient rationing and T-S in the water layers. Directly sinking phytoplankton cells are major contributors to surface carbon export and an important component of ocean carbon sink (Boyd and Newton, 1999). The phytoplankton cells can regulate their sinking rates in a variety of ways, such as the physiological state of themselves (Eppley et al., 1967), morphology of themselves (Pitcher et al., 1989), light (Bienfang, 1981) and environmental factors such as temperature and nutrients (Titman and Kilham, 1976).

4.3 Vertical stratification determined the vertical distribution of phytoplankton

The WPO is a oligotrophic area with strong stratification. We found that the interannual variation of phytoplankton was not significant. It remained stably oligotrophic, and the vertical stratification structure determined that of environmental resources such as nutrients, thus forming four contrasting environments, each with its characteristic phytoplankton community structure. Comparative analysis of the phytoplankton community composition of the four groups showed that the phytoplankton was mainly strongly affected by the vertical stratification, which corresponds to previous research (Bouman et al., 2011; Hidalgo et al., 2014; Mojica et al., 2015). Vertical stratification limits the replenishment of nutrients from the deep layer below the thermocline, which affects the N: P ratio, and restricts vertical migration as well as physiologically affecting the vertical structure of phytoplankton growth and mortality (Gupta et al., 2020).

In the present study, *Trichodesmium* was the dominant cyanobacterial species. Marine *Trichodesmium* is considered the most critical autotrophic nitrogen-fixing cyanobacteria (Dugdale et al., 1961). *Trichodesmium* can be divided into two forms: clusters and free filaments. *Trichodesmium* thrives in waters above 20 °C, and has a special cellular air sac structure that allows it to move vertically within the upper 100 m of the ocean water column (Laroche et al., 2005). In the process of water blooms formed by *Trichodesmium*, a large amount of nitrogen is often fixed in a relatively short period of time. Therefore, the study of the nitrogen fixation rate of *Trichodesmium* is crucial for estimating the rate of nitrogen fixation in the ocean (Karl et al., 2002). Previous studies have not clarified which factors are the main causes of *Trichodesmium* growth (possibly temperature, wind, iron, phosphorus, etc.) (Capone et al., 1997; Chang et al., 2000; Sañudo-Wilhelmy et al., 2001; Karl et al., 1997). Many researchers have proposed that temperature is the most important factor affecting the growth of *Trichodesmium* (Capone et al., 1999; Kustka et al., 2002). However, we suggest that there is no single positive correlation between temperature and *Trichodesmium* growth, which also is consistent with the study of Chang (2000). In the tropical WPO, where the surface temperatures all exceeded 20 °C, the abundance of *Trichodesmium* in areas with higher temperatures

(Groups A and B) was higher than in those with lower temperatures (Groups C and D). Temperature not only directly affected phytoplankton growth, but also indirectly affected phytoplankton growth and abundance by regulating VSI to drive the nutrient ratio (N: P) (Figure 10).

Previous models and field experiments have shown that the species composition of phytoplankton communities is significantly affected by vertical turbulent mixing changes (Huisman et al., 2004). A strong coupling exists among the nutrient supply rate, the photosynthetic performance of phytoplankton (Bouman et al., 2006), the phytoplankton biomass and primary production, particularly in eutrophic areas (Richardson et al., 2019). The vertical stratification index reflects the potential effects of vertical stratification on various physical and chemical processes, such as regulating the utilization of light and nutrients in the ocean, which in turn affects phytoplankton dynamics. The results of the present study showed that from the equator to the north, the VSI decreases as the latitude increases, and the phytoplankton community structure changes from cyanobacteria to diatoms. Phytoplankton abundance was significantly different in the water layer above the SCM. The water layer below the SCM tended to be stable. The surface phytoplankton abundance was usually greater than that of the SCM layer, and was related to the surface layer of *Trichodesmium*. Our results demonstrate that the highly stratified region was more suitable for the growth of *Trichodesmium*, while the region with low vertical stratification seems to be more conducive to diatoms and dinoflagellates (Figures 6 and 8). Due to their low mobility and high potential growth rate, diatoms can reproduce rapidly in mixed water with high nutrient content (Tilman et al., 1986). The weak vertical stratification of Group C and D regions (Figure 9b) leads to relative homogeneity of temperature, salinity, density, and nutrients in the upper part of 200 m in the vertical direction (Perez et al., 2006). The vertical distribution of zooplankton has shown that vertical stratification can hinder the migration of small zooplankton populations and indicate different grazing pressures (Mitra et al., 2005; Long et al., 2021). Further research should consider the difference in predation pressure of different zooplankton predators on the composition of the phytoplankton community in different regions. Phytoplankton stratification may cause thin-layer algal blooms and other phenomena, and the influence of phytoplankton stratification can be investigated in further investigated.

5 Conclusions

This study investigated the phytoplankton community structure of the WPO in the autumn of 2016, 2017, and 2018. The WPO is a oligotrophic ocean with a weak water exchange capacity owing to the thermocline and severe stratification in the upper seawater layer. The phytoplankton community structure mainly consisted of cyanobacteria, diatoms, and dinoflagellates, while the abundance of Chrysophyceae was low. In terms of spatial distribution, phytoplankton abundance was high from the equatorial region to 10 °N, and decreased with increasing latitude. Phytoplankton showed a high variation in the vertical distribution. The potential influences of physicochemical parameters on phytoplankton abundance were analyzed by Structural Equation Model (SEM) to determine nutrient ratios driven by vertical stratification to regulate phytoplankton community structure in a typical oligotrophic sea area. Regions with strong vertical stratification (Groups A and B) were more favorable for cyanobacteria, whereas weak vertical stratification (Groups C and D) was more conducive to diatoms and dinoflagellates.

Funding: This research was financially supported by the National Key Research and Development

Project of China (2019YFC1407805), the National Natural Science Foundation of China (41876134, 41676112 and 41276124), the Tianjin 131 Innovation Team Program (20180314), and the Changjiang Scholar Program of Chinese Ministry of Education (T2014253) to Jun Sun.

Data availability: All data are available upon request by contacting the correspondence author.

Author Contributions: ZC performed the analyses and wrote the article. JS, TG, YQW, and GCZ conceived the research idea, directed the project, and supported the article revision.

Competing interests: The authors declare that they have no conflict of interest.

Acknowledgments: We thank the Natural Science Foundation for its support of the Northwest Pacific voyage for sampling and field experiments. Samples were collected onboard of R/V *Kexue* implementing the open research cruise (voyage number: NORC2016-09, NORC2017-09 and NORC2018-09) supported by NSFC Shiptime Sharing Project. Thank you to all the staff of "*Kexue*" for their help. Thanks for the CTD data provided by Dongliang Yuan Physical Oceanography Research Group, Institute of Oceanography, Chinese Academy of Sciences.

References

Bertilsson, S., Berglund, O., Karl, D. M., and Chisholm, S. W.: Elemental composition of marine *Prochlorococcus* and *Synechococcus*, Implications for the ecological stoichiometry of the sea, Limnol. Oceanogr., 48, 1721–1731, https://doi.org/10.4319/lo.2003.48.5.1721, 2003.

Bienfang P. K.: SETCOL – a technologically simple and reliable method for measuring phytoplankton sinking rates, Canadian Journal of Fisheries and Aquatic Sciences, 38, 1289–1294, https://doi.org/10.1139/f81-173, 1981.

Bouman, H. A., Ulloa, O., Barlow, R., Li, W. K. W., Platt, T., Zwirglmaier, K., Scanlan, D. J., and Sathyendranath, S.: Water-column stratification governs the community structure of subtropical marine picophytoplankton, Environmental microbiology reports, 3, 473–482, https://doi.org/10.1111/j.1758-2229.2011.00241.x, 2011.

Bouman, H. A., Ulloa, O., Scanlan, D. J., Zwirglmaier, K., Li, W., Platt, T., Stuart, V., Barlow, R., Leth, O., Clementson, L., Lutz, V., Fukasawa, M., Watanabe, S., and Sathyendranath, S.: Oceanographic basis of the global surface distribution of *Prochlorococcus* ecotypes, Science, 312 (5775), 918–921, https://doi.org/10.1126/science.1122692, 2006.

Boyd, P. W. and Newton, P. P.: Does planktonic community structure determine downward particulate organic carbon flux in different oceanic provinces?, Deep-Sea Research Part I, 46, 63–91, https://doi.org/10.1016/S0967-0637(98)00066-1, 1999.

Capone, D., and Carpente, E.: Nitrogen fixation by marine cyanobacteria: historical and global perspectives, Bulletin De Linstitut Océanographique, 19, 235–256, 1999.

Capone, D. G., Zehr, J. P., Paerl, H. W., Bergman, B., and Carpenter, E. J.: Trichodesmium, a globally significant marine Cyanobacterium, Science, 276, 1221–1229, https://doi.org/10.1126/science.276.5316.1221, 1997.

Carlson, C. A.: Production and removal processes, Biogeochemistry of marine dissolved organic matter, 91–151, https://doi.org/10.1016/B978-012323841-2/50006-3, 2002.

Chang, J., Chiang, K. P., and Gong, G. C.: Seasonal variation and cross-shelf distribution of the nitrogen-fixing cyanobacterium, *Trichodesmium*, in southern East China Sea, Continental Shelf Research, 20, 479–492, https://doi.org/10.1016/S0278-4343(99)00082-5, 2000.

Chen, M., Lu, Y., Jiao, N., Tian, J., Kao, S. J., and Zhang, Y.: Biogeographic drivers of diazotrophs in the western Pacific Ocean, Limnol. Oceanogr., 9999, 1–19, https://doi.org/10.1002/lno.11123, 2019.

Chen, Y., Sun, X., and Zhu, M.: Net-phytoplankton communities in the Western Boundary Currents and their environmental correlations, Chinese Journal of Oceanology and Limnology, https://doi.org/10.1007/s00343-017-6261-8, 2018a.

Chen, Z., Sun, J., and Zhang, G.: Netz-phytoplankton community structure of the tropical Western Pacific Ocean in summer 2016, Marine science, 42, 114–130, https://doi.org/10.11759//hykx20180331002, 2018b.

Cronin, M. F., Bond, N. A., Farrar, J. T., Ichikawa, H., Jayne, S. R., Kawai, Y., Konda, M., Qiu, B., Rainville, L., and Tomita, H.: Formation and erosion of the seasonal thermocline in the Kuroshio Extension recirculation gyre, Deep-Sea Research II, 85, 62–74, https://doi.org/10.1016/j.dsr2.2012.07.018, 2013.

Dai, M., Wang, L., Guo, X., Zhai, W., Li, Q., He, B., and Kao, S. J.: Nitrification and inorganic nitrogen distribution in a large perturbed river/estuarine system: the Pearl River Estuary, China, Biogeosciences, 5, 1227–1244, https://doi.org/10.5194/bg-5-1227-2008, 2008.

Dai, S., Zhao, Y., Li, X., Wang, Z., Zhu, M., Liang, J., Liu, H., Tian, Z., and Sun, X.: The seamount effect on phytoplankton in the tropical western Pacific, Marine Environmental Research, 162, https://doi.org/10.1016/j.marenvres.2020.105094, 2020.

Doney, S. C.: Plankton in a warmer world, Nature, 444, 695–696, https://doi.org/10.1038/444695a, 2006.

Duce, R. A., and Tindale, N. W.: Atmospheric transport of iron and its deposition in the ocean, Limnol. Oceanogr., 36: 1715–1726, 1991.

Dugdale, R. C., Menzel, D. W., and Ryther, J. H.: Nitrogen fixation in the Sargasso Sea, Deep Sea Research, 7, 297–300, https://doi.org/10.1016/0146-6313(61)90051-X, 1961.

Egge, J. K.: Are diatoms poor competitors at low phosphate concentrations?, Journal of Marine Systems, 16, 191–198, https://doi.org/10.1016/S0924-7963(97)00113-9, 1998.

Eppley, R. W., Holmes, R. W., and Strickland J. D. H.: Sinking rates of marine phytoplankton measured with a fluorometer, Journal of Experimental Marine Biology and Ecology, 1, 191– 208, https://doi.org/10.1016/0022-0981(67)90014-7, 1967.

Falkowski, P. G., Barber, R. T., and Smetacek, V.: Biogeochemical controls and feedbacks on ocean primary production, Science, 281, 200–206, doi:10.1126/science.281.5374.200, 1998.

Field, C. B., Behrenfeld, M. J., Randerson, J. T., and Falkowski, P.: Primary production of the biosphere: Integrating terrestrial and oceanic components, Science, 281, 237–240, doi:10.1126/science.281.5374.237, 1998.

Fogg, G. E.: The ecological significance of extracellular products of phytoplankton photosynthesis, Botanica Marina, 26, 3–14, https://doi.org/10.1515/botm.1983.26.1.3, 1983.

Gao, K., Beardall, J., Häder, D. P., Hall-Spencer, J. M., Gao, G., and Hutchins, D. A.: Effects of ocean acidification on marine photosynthetic organisms under the concurrent influences of warming, UV radiation, and deoxygenation, Frontiers in marine science, 6, https://doi.org/10.3389/fmars.2019.00322, 2019.

Geider, R. J., Maclntyre, H. L., and Kana, T. M.: A dynamic regulatory model of phytoplanktonic acclimation to light, nutrients, and temperature: Limnol. Oceanogr., 43, 679–694, https://doi.org/10.2307/2839077, 1998.

Goldman, J. C., Mccarthy, J. J., and Peavey, D. G.: Growth rate influence on the chemical composition of phytoplankton in oceanic waters, Nature, 279, 210–215, https://doi.org/10.1038/279210a0, 1979.

Grasshoff, K., Kremling, K., and Ehrhardt, M.: Methods of Seawater Analysis, third, completely revised and extended edition.Weinheim: Wiley-VCH, 193–198, 1999.

Grosskopf, T., Mohr, W., Baustian, T., Schunck, H., Gill, D., Kuypers, M., Lavik, G., Schmitz, R. A., Wallace, D., and Laroche, J.: Doubling of marine dinitrogen-fixation rates based on direct measurements, Nature, 488, 361–364, https://doi.org/10.1038/nature11338, 2012.

Guo, S., Feng, Y., Lei, W., Dai, M., Liu, Z., Bai, Y., and Sun, J.: Seasonal variation in the phytoplankton community of a continental-shelf sea: the East China Sea, Marine Ecology Progress, 103–126, https://doi.org/10.3354/meps10952, 2014.

Gupta, A. S., Thomsen, M., Benthuysen J. A., Hobday, A. J., Oliver, E., Alexander, L. V., Burrows, M. T., Donat, M. G., Feng, M., Holbrook, N. J., Perkins-Kirkpatrick, S., Moore, P. J., Rodrigues, R.

R., Scannell, H. A., Taschetto, A. S., Ummenhofer, C. C., Wernberg, T., and Smale, D. A.: Drivers and impacts of the most extreme marine heatwaves events, Scientific reports, 10, https://doi.org/10.1038/s41598-020-75445-3, 2020.

Hansell, D. A. and Feely, R. A.: Atmospheric Intertropical Convergence impacts surface ocean carbon and nitrogen biogeochemistry in the western tropical Pacific, Geophysical Research Letters, 27, 1013–1016, https://doi.org/10.1029/1999gl002376, 2000.

Hidalgo, M., Reglero, P., Álvarez-Berastegui, D., Torres, A. P., Álvarez, I., Rodriguez, J. M., Carbonell, A., Zaragoza, N., Tor, A., Goñi, R., Mallol, S., Balbín, R., and Alemany, F.: Hydrographic and biological components of the seascape structure the meroplankton community in a frontal system, Marine Ecology Progress Series, 505, 65–80, https://doi.org/10.3354/meps10763, 2014.

Hillebrand, H., Steinert, G., Boersma, M., Malzahn, A., Meunier, C. L., Plum, C., and Ptacnik, R.: Goldman revisited: Faster-growing phytoplankton has lower N: P and lower stoichiometric flexibility, Limnol. Oceanogr., 58, 2076–2088, doi:10.4319/lo.2013.58.6.2076, 2013.

Huang, B., Ou, L., Hong, H., Luo, H., and Wang, D.: Bioavailability of dissolved organic phosphorus compounds to typical harmful dinoflagellate Prorocentrum donghaiense Lu, Marine Pollution Bulletin, 51: 838–844, https://doi.org/10.1016/j.marpolbul.2005.02.035, 2005.

Huisman, J., Sharples, J., Stroom, J. M., Visser, P. M., Kardinaal, W. E. A., Verspagen, J. M. H., and Sommeijer, B.: Changes in turbulent mixing shift competition for light between phytoplankton species, Ecology, 85, 2960–2970, https://doi.org/10.1890/03-0763, 2004.

Jin, D., and Chen, J.: Chinese Marine Planktonic Diatoms, Shanghai Scientific & Technical Press, 1–230, 1965.

Karl, D. M., Björkman, K. M., Dore, J. E., Fujieki, L., Hebel, D. V., Houlihan, T., Letelier, R. M., and Tupas, L. M.: Ecological nitrogen-to-phosphorus stoichiometry at station ALOHA. Deep-Sea Research II, 48, 1529–1566, https://doi.org/10.1016/S0967-0645(00)00152-1, 2001.

Karl, D. M., Hebel, D. V., Björkman, K., and Letelier, R. M.: The role of dissolved organic matter release in the productivity of the oligotrophic North Pacific Ocean, Limnol. Oceanogr., 43, 1270–1286, https://doi.org/10.4319/lo.1998.43.6.1270, 1998.

Karl, D., Michaels, A., Bergman, B., Capone, D., Carpenter, E., Letelier, R., Lipschultz, F., Paerl, H., Sigman, D., and Stal, L.: Dinitrogen fixation in the world's oceans, Biogeochemistry, 57/58, 47–98, https://doi.org/10.1007/978-94-017-3405-9_2, 2002.

Karl, D. M., and Tien, G.: Temporal variability in dissolved phosphorus concentrations in the subtropical North Pacific Ocean, Marine Chemistry, 56: 77–96, https://doi.org/10.1016/S0304-4203(96)00081-3, 1997.

Kustka, A., Carpenter, E. J., and Sañudo-Wilhelmy, S. A.: Iron and marine nitrogen fixation: progress and future directions, Research in Microbiology, 153, 255–262, https://doi.org/10.1016/S0923-2508(02)01325-6, 2002.

Laroche, J., and Breitbarth, E.: Importance of the diazotrophs as a source of new nitrogen in the ocean, Journal of Sea Research, 53, 67–91, https://doi.org/10.1016/j.seares.2004.05.005, 2005.

Li, Q., Legendre, L., and Jiao, N. Z.: Phytoplankton responses to nitrogen and iron limitation in the tropical and subtropical Pacific Ocean, Journal of Plankton Research, 37, 306–319, https://doi.org/10.1093/plankt/fbv008, 2015.

Liu, D. Y., Sun, J., and Qian, S. B.: Planktonic dinoflagellate in Ryukyu-gunto and its adjacent waters-species composition and their abundance distribution in summer 1997, Collected Works of Chinese Oceanography, 2000.

Lin, G. M., Chen, Y. H., Huang, J., Wang, Y. G., Ye, Y. Y., and Yang, Q. L.: Regional disparities of phytoplankton in relation to different water masses in the Northwest Pacific Ocean during the spring and summer of 2017, Acta Oceanologica Sinica, 39, https://doi.org/10.1007/s13131-019-1511-6, 2020.

Long, Y., Noman, A., Chen, D. W., Wang, S. H., Yu, H., Chen, H. T., Wang, M., and Sun, J.: Western pacific zooplankton community along latitudinal and equatorial transects in autumn 2017 (northern hemisphere), Diversity, 13, 58, https://doi.org/10.3390/d13020058, 2021.

Luo, Y. W., Doney, S. C., Anderson, L. A., Benavides, M.,Berman-Frank, I. Bode, A., Bonnet, S., Bostrom, K. H., Boettjer, D., Capone, D. G., and Zehr, J. P.: Database of diazotrophs in global ocean: abundance, biomass and nitrogen fixation rates, Earth System Science Data, 4, 47–73, https://doi.org/10.5194/essd-4-47-2012, 2012.

Mena, C., Reglero, P., Hidalgo, M., Sintes, E., Santiago, R., Martín, M., Moyà, G., and Balbín, R.: Phytoplankton community structure is driven by stratification in the oligotrophic mediterranean sea, Frontiers in microbiology, 10, https://doi.org/10.3389/fmicb.2019.01698, 2019.

Mitra, A. and Flynn, K. J.: Predator-prey interactions: is 'ecological stoichiometry' sufficient when good food goes bad?, Journal of Plankton Research, 27, 393–399, https://doi.org/10.1093/plankt/fbi022, 2005.

Mojica, K. D. A., van de Poll, W. H., Kehoe, M., Huisman, J., Timmermans, K. R., Buma, A. G. J., van der Woerd, H. J., Hahn-Woernle, L., Dijkstra, H. A., and Brussaard, C. P. D.: Phytoplankton community structure in relation to vertical stratification along a north-south gradient in the Northeast Atlantic Ocean, Limnology and Oceanography, 60, 1498–1521, https://doi.org/10.1002/lno.10113, 2015.

Oksanen, J. F., Blanchet, F. G., Friendly, M., Kindt, R., Legendre, P., McGlinn, D., Minchin, P. R.,

O'Hara, R. B., Simpson, G. L., Solymos, P., Stevens, M. H., Szoecs, E., and Wagner, H.: vegan: Community Ecology Package, 2020.

Pai, S. C., Tsau, Y. J., and Yang, T. I.: PH and buffering capacity problems involved in the determination of ammonia in saline water using the indophenol blue spectrophotometric method, Analytica Chimica Acta, 434, 209–216, https://doi.org/10.1016/S0003-2670(01)00851-0, 2001.

Pérez, V., Fernández, E., Marañón, E., Morán, X. A. G., and Zubkov, M. V.: Vertical distribution of phytoplankton biomass, production and growth in the Atlantic subtropical gyres, Deep-Sea Research Part I, 53, 1616–1634, https://doi.org/10.1016/j.dsr.2006.07.008, 2006.

Pitcher G. C., Walker D. R., and Mitchell-Innes B. A.: Phytoplankton sinking rate dynamics in the southern Bengurla upwelling system, Marine Ecology Progress Series, 55: 261–269, https://doi.org/10.3354/meps055261, 1989.

Qiu, B., Chen, S. M., and Hacker, P.: Synoptic‐scale air–sea flux forcing in the western North Pacific: Observations and their impact on SST and the mixed layer, Journal of Physical Oceanography, 34, 2148–2159, https://doi.org/10.1175/1520-0485(2004)0342.0.CO;2, 2004.

Redfield, A. C., Ketchum, B. H., and Richards, F. A.: The influence of organisms on the composition of sea-water, Sea, 26–77, https://doi.org/10.1061/40640(305)14, 1963.

Richardson, K., and Bendtsen, J.: Vertical distribution of phytoplankton and primary production in relation to nutricline depth in the open ocean, Marine Ecology Progress Series, 620, 33–46, https://doi.org/10.3354/meps12960, 2019.

Sañudo-Wilhelmy, S. A., Kustka, A. B., Gobler, C. J., Hutchins, D. A., Yang, M., Lwiza, K., Burns, J., Capone, D. G., Raven, J. A., Carpenter, E. J.: Phosphorus limitation of nitrogen fixation by *Trichodesmium* in the central Atlantic Ocean, Nature, 411: 66–69, https://doi.org/10.1038/35075041, 2001.

Schindler, D. W.: Ecological stoichiometry: The biology of elements from molecules to the biosphere, Nature, 423, 225–226, https://doi.org/10.1038/423225b, 2003.

Smayda T J.: Harmful algal blooms: their ecophysiology and general relevance to phytoplankton blooms in the sea, Limnology and Oceanography, 42: 1137–1153, https://doi.org/10.2307/2839007, 1997.

Sohm, J. A., Webb, E. A., and Capone, D. G.: Emerging patterns of marine nitrogen fixation, Nature Reviews Microbiology, 9, 499–508, https://doi.org/10.1038/nrmicro2594, 2011.

Stoecker, D. K.: Mixotrophy among dinoflagellates, Journal Eukaryot Microbiol, 46: 397–401, https://doi.org/10.1111/j.1550-7408.1999.tb04619.x, 1999.

Sun, J., Liu, D. Y., and Qian, S. B.: A Quantative Research and Analysis Method for Marine Phytoplankton :An Introduction to Utermöhl Method and Its Modification, Journal of oceanography of Huanghai &Bohai seas, 20, 105–112, 2002a.

Sun, J., and Liu, D. Y.: The Preliminary Notion on Nomenclature of Common Phytoplankton in China Sea Waters, Oceanologia Et Limnologia Sinica, 33, 271–286, https://doi.org/10.1088/1009-1963/11/5/313, 2002b.

Sun, J., Liu, D. Y., and Qian, S. B.: Planktonic diatoms in Ryukyu-gunto and its adjacent waters-species composition and abundance distribution in summer 1997, Collected Works of Chinese Oceanography, 2000.

Titman D., and Kilham P.: Sinking in freshwater phytoplankton: some ecological implications of cell nutrient status and physical mixing processes, Limnology and Oceanography, 21, 409–417, https://doi.org/10.4319/lo.1976.21.3.0409, 1976.

Tilman, D., Kiesling, R., Sterner, R., Kilham, S. S., and Johnson, F. A.: Green, bluegreen and diatom algae: taxonomic differences in competitive ability for phosphorus, silicon and nitrogen, Arch Hydrobiol, 106, 473–485, https://doi.org/10.1029/WR022i007p01162, 1986.

Yamaguchi, R., Suga, T., Richards, K. J., and Qiu, B.: Diagnosing the development of seasonal stratification using the potential energy anomaly in the North Pacific, Climate Dynamics, 53, 4667–4681, https://doi.org/10.1007/s00382-019-04816-y , 2019.

Yamaji, I.: Illustrations of the Marine Plankton of Japan, Tpkyo: Hoikusha Press, 1-158, 1991.

Zehr, J. P.: Nitrogen fixation by marine cyanobacteria, Trends in Microbiology, 19, 162–173, https://doi.org/10.1016/j.tim.2010.12.004, 2011.

Zhang, Q.: Relationship between the precipitation in the rainy season in north China and the tropical western pacific warm pool and Kuroshio, Plateau Meteorology, 18, 575–583, 1999.

Zhu, J., Zheng, Q. A., Hu, J. Y., Lin, H. Y., Chen, D. W., Chen, Z. Z., Sun, Z. Y., Li, L. Y., and Kong, H.: Classification and 3-D distribution of upper layer water masses in the northern South China Sea, Acta Oceanol. Sin., 38, 126–135, https://doi.org/10.1007/s13131-019-1418-2, 2019.